

The $n + 1$ distinct eigenvalues are symmetric around zero, equidistant and range from $-n$ to n . Hence for even n , they are $n + 1$ consecutive even integers, while for odd n they are $n + 1$ consecutive odd integers.

Remark 1. *The eigenvectors of the matrix C_n are also known, they can be expressed in terms of the Krawtchouk orthogonal polynomials [16].*

As the eigenvalues of (2) are known explicitly and because of the elegant and simple structure of both matrix and spectrum, C_n is a standard test matrix for numerical eigenvalue computations (see e.g. example 7.10 in [9]), and part of some standard test matrix toolboxes (e.g. [10]). In MATLAB, C_n can be produced from the gallery of test matrices using `gallery('clement', n+1)`. The Clement matrix also appears in several applications, e.g. as the transition matrix of a Markov chain [1], or in biogeography [11].

General tridiagonal matrices with closed form eigenvalues are rare, most examples being just variations of the tridiagonal matrix with fixed constants a , b and c on the subdiagonal, diagonal and superdiagonal respectively [6, 21]. In this paper we present appealing two-parameter extensions of C_n with closed form eigenvalues. These extensions first appeared in a different form in the paper [17] as a special case of a class of matrices related to orthogonal polynomials. Special cases of these matrices were originally encountered in the context of finite quantum oscillator models (e.g. [12]) and their classification led to the construction of new interesting models [18]. Here, we feature them in a simpler, more accessible form which immediately illustrates their relation with C_n . Moreover, we consider some specific parameter values which yield interesting special cases.

Another purpose of this paper is to demonstrate by means of some numerical experiments the use of these extensions of C_n as test matrices for numerical eigenvalue computations. Hereto, we examine how accurately the inherent MATLAB function `eig()` is able to compute the eigenvalues of our test matrices compared to the exact known eigenvalues. An interesting feature of the new class of test matrices is that they include matrices with double eigenvalues for specific parameter values.

In section 2 we present in an accessible form the two-parameter extensions of the Clement matrix. We state the explicit and rather simple form of their eigenvalues which makes them potentially interesting examples of eigenvalue test matrices. In section 3 we consider some specific parameter values for the new classes of test matrices which yield interesting special cases. In section 4 we display some numerical results regarding the use of these extensions as test matrices for numerical eigenvalue computations. This is done by looking at the relative error when the exact known eigenvalues are compared with those computed using the inherent MATLAB function `eig()`.

2. New test matrices

Now, we consider the following extension of the matrix (2), by generalizing its entries (1) to:

$$h_{k,k+1} = \begin{cases} k & \text{if } k \text{ even} \\ k + a & \text{if } k \text{ odd} \end{cases} \quad \text{and} \quad h_{n+2-k,n+1-k} = \begin{cases} k & \text{if } k \text{ even} \\ k + b & \text{if } k \text{ odd} \end{cases} \quad (4)$$

where we introduce two parameters a and b (having a priori no restrictions). We will denote this extension by $H_n(a, b)$. For n even, the matrix $H_n(a, b)$ is given by (5). Note in particular that the first entry of the second row is $h_{2,1} = n$ and contains no parameter, and the same for $h_{n,n+1} = n$. For odd n , the matrix (7) has entries $h_{2,1} = n + b$ and $h_{n,n+1} = n + a$ which now do contain parameters, contrary to the even case.

The reason for considering this extension is that, similar to (3) for C_n , we also have an explicit expression for the spectrum of $H_n(a, b)$, namely:

This matrix is also implemented in MATLAB, namely as `gallery('clement', n+1, 1)`. For the extension $H_n(a, b)$, the entries of its symmetric form $\tilde{H}_n(a, b)$ are

$$\tilde{h}_{k,k+1}^e = \tilde{h}_{k+1,k}^e = \begin{cases} \sqrt{k(n+1-k+b)} & \text{if } k \text{ even} \\ \sqrt{(k+a)(n+1-k)} & \text{if } k \text{ odd} \end{cases}$$

for n even and $k \in \{1, \dots, n\}$, while for n odd we have

$$\tilde{h}_{k,k+1}^o = \tilde{h}_{k+1,k}^o = \begin{cases} \sqrt{k(n+1-k)} & \text{if } k \text{ even} \\ \sqrt{(k+a)(n+1-k+b)} & \text{if } k \text{ odd} \end{cases}$$

for $k \in \{1, \dots, n\}$.

The above theorems are now proved using a property of the dual Hahn polynomials, which are defined in terms of the generalized hypergeometric series as follows [14]

$$R_n(\lambda(x); \gamma, \delta, N) = {}_3F_2 \left(\begin{matrix} -x, x + \gamma + \delta + 1, -n \\ \gamma + 1, -N \end{matrix}; 1 \right). \quad (11)$$

The dual Hahn polynomials satisfy a discrete orthogonality relation, see [17, (2.7)], and we denote the related orthonormal functions as $\tilde{R}_n(\lambda(x); \gamma, \delta, N)$.

Lemma 1. *The orthonormal dual Hahn functions satisfy the following pairs of recurrence relations:*

$$\begin{aligned} & \sqrt{(n+1+\gamma)(N-n)}\tilde{R}_n(\lambda(x); \gamma, \delta, N) - \sqrt{(n+1)(N-n+\delta)}\tilde{R}_{n+1}(\lambda(x); \gamma, \delta, N) \\ & = \sqrt{x(x+\gamma+\delta+1)}\tilde{R}_n(\lambda(x-1); \gamma+1, \delta+1, N-1), \end{aligned} \quad (12)$$

$$\begin{aligned} & -\sqrt{(n+1)(N-n+\delta)}\tilde{R}_n(\lambda(x-1); \gamma+1, \delta+1, N-1) + \sqrt{(n+2+\gamma)(N-n-1)} \\ & \times \tilde{R}_{n+1}(\lambda(x-1); \gamma+1, \delta+1, N-1) = \sqrt{x(x+\gamma+\delta+1)}\tilde{R}_{n+1}(\lambda(x); \gamma, \delta, N) \end{aligned} \quad (13)$$

and

$$\begin{aligned} & \sqrt{(n+1+\gamma)(N-n+\delta)}\tilde{R}_n(\lambda(x); \gamma, \delta, N) - \sqrt{(n+1)(N-n)}\tilde{R}_{n+1}(\lambda(x); \gamma, \delta, N) \\ & = \sqrt{(x+\gamma+1)(x+\delta)}\tilde{R}_n(\lambda(x); \gamma+1, \delta-1, N), \end{aligned} \quad (14)$$

$$\begin{aligned} & -\sqrt{(n+1)(N-n)}\tilde{R}_n(\lambda(x); \gamma+1, \delta-1, N) + \sqrt{(n+2+\gamma)(N-n+\delta-1)} \\ & \times \tilde{R}_{n+1}(\lambda(x); \gamma+1, \delta-1, N) = \sqrt{(x+\gamma+1)(x+\delta)}\tilde{R}_{n+1}(\lambda(x); \gamma, \delta, N). \end{aligned} \quad (15)$$

Proof.

The first two relations follow from the case dual Hahn I of [17, Theorem 1] multiplied by the square root of the weight function and norm squared, and similarly the last two from the case dual Hahn III. \square

Proof of Theorem 2.

Let n be an even integer, say $n = 2m$, and let a and b be real numbers greater than -1 . Take $k \in \{1, \dots, m\}$ and let $U_{\pm k} = (u_1, \dots, u_{n+1})^T$ be the column vector with entries

$$u_l = \begin{cases} (-1)^{(l-1)/2} \tilde{R}_{(l-1)/2}(\lambda(k); \frac{a-1}{2}, \frac{b-1}{2}, m) & \text{if } l \text{ odd} \\ \pm (-1)^{l/2-1} \tilde{R}_{l/2-1}(\lambda(k-1); \frac{a+1}{2}, \frac{b+1}{2}, m-1) & \text{if } l \text{ even.} \end{cases}$$

We calculate the entries of the vector $\tilde{H}_n(a, b)U_{\pm k}$ to be

$$(\tilde{H}_n(a, b)U_{\pm k})_l = \tilde{h}_{l,l-1}^e u_{l-1} + \tilde{h}_{l,l+1}^e u_{l+1}.$$

with imaginary parts when $a > 21$ or $a < -2.5$. Moreover, the relative error for the computed eigenvalues, shown in figures 2, increases as a approaches the region where eigenvalues with imaginary parts are found. In this latter region, the size of the relative error is of course due to the presence of imaginary parts which do not occur in the theoretical exact expression for the eigenvalues. As a reference, the relative error for C_{100} is 3.6612×10^{-5} , while that for $H_{100}(20)$ is 1.1471×10^{-3} and 4.9444×10^{-3} for $H_{100}(20.97)$.

For n odd, $H_n(a)$ has the eigenvalues (18), which dependent on the parameter a but are real for every real number a . Nevertheless, even for a small dimension such as $n = 11$, eigenvalues with (small) imaginary parts are found when a equals $-2, -4, -6$ or -8 . This produces a relative error of order 10^{-8} , while for other values of a (and for the Clement matrix) the relative error is of order 10^{-15} , near machine precision. For $H_{101}(a)$, the largest imaginary part of the computed eigenvalues is portrayed in figure 3, together with the relative error. MATLAB finds eigenvalues with imaginary parts when $-100 \leq a < -1.5$. These findings correspond to the region where double eigenvalues occur as mentioned in the previous section. The relative error is largest around this region and is several orders smaller when moving away from this region. As a reference, the relative error for C_{101} is 3.6881×10^{-5} , while that for $H_{101}(-1.75)$ is 1.4840×10^{-3} . Finally, we note that eigenvalues with imaginary parts also appear when a is extremely large, i.e. $a > 10^{10}$ or $a < -10^{10}$.

Next, we consider the general setting where we have two parameters a and b , starting with the case where n is even. Although the two parameters a and b occur symmetric in (6) and in the matrix (5) itself, there are some disparities in the numerical results. From the expression for the eigenvalues (6) we see that they are real when the parameters satisfy $a + b > -2$. However,

- when a is a negative number less than -2 , MATLAB finds eigenvalues with imaginary parts for almost all values of b .
- for negative values of b , no imaginary parts are found as long as $a + b > -2$.
- For positive values of a , eigenvalues with imaginary parts are found when b gets sufficiently large, as illustrated in figure 4.
- For positive values of b the opposite holds: eigenvalues with imaginary parts are found when a is comparatively small, see figure 5.

In the case where n is odd, similar results hold for positive parameter values for a and b , as shown in figure 6 for example. For negative parameter values we have a different situation, as the eigenvalues (8) can become imaginary if the two factors have opposite sign. When $a < -n$ and $b < -n$, the eigenvalues (8) are real again and the behaviour mimics that of the positive values of a and b . The picture we get is a mirror image of figure 6.

The reason for this disparity between the seemingly symmetric parameters a and b is that the QR algorithm wants to get rid of subdiagonal entries in the process of creating an upper triangular matrix. As a consequence, the numerical computations are much more sensitive to large values of b as it resides on the subdiagonal. This is showcased in figures 4, 5 and 6. Most important is the sensitivity on the extra parameters (a or a and b) which makes them appealing as test matrices.

It would be interesting future work if these new eigenvalue test matrices were to be used to test also numerical algorithms for computing eigenvalues designed specifically for matrices having multiple eigenvalues [8], being tridiagonal [15], or symmetric and tridiagonal [4].

References

- [1] E.A. Abdel-Rehim, From the Ehrenfest model to time-fractional stochastic processes. *J. Comput. Appl. Math.* **233** (2009), no. 2, 197-207.
- [2] R. Bevilacqua, E. Bozzo, The Sylvester-Kac matrix space, *Linear Algebra Appl.* **420** (2009), 3331-3138.
- [3] T. Boros, P. Rózsa, An explicit formula for singular values of the Sylvester-Kac matrix, *Linear Algebra Appl.* **421** (2007), 407-416.
- [4] P. Brockman, T. Carson, Y. Cheng, T.M. Elgindi, K. Jensen, X. Zhoun, M.B.M. Elgindi, Homotopy method for the eigenvalues of symmetric tridiagonal matrices. *J. Comput. Appl. Math.* **237** (2013), no. 1, 644-653.
- [5] P.A. Clement, A class of triple-diagonal matrices for test purposes, *SIAM Review* **1** (1959), 50-52.

- [6] J.A. Cuminato, S. McKee, A note on the eigenvalues of a special class of matrices. *J. Comput. Appl. Math.* **234** (2010), no. 9, 2724-2731.
- [7] A. Edelman, E. Kostlan, The road from Kac's matrix to Kac's random polynomials. In Proceedings of the 1994 SIAM Applied Linear Algebra Conference (Philadelphia, 1994), J. Lewis, Ed., SIAM, pp. 503–507. 1994.
- [8] A. Galántai, C.J. Hegedűs, Hymans method revisited. *J. Comput. Appl. Math.* **226** (2009), no. 2, 246–258.
- [9] R.T. Gregory, D.L. Karney, A collection of matrices for testing computational algorithms. Wiley-Interscience A Division of John Wiley & Sons, Inc., New York-London-Sydney 1969 ix+154 pp.
- [10] N. Higham, The Test Matrix Toolbox for Matlab, *Numerical Analysis Report No. 237*, University of Manchester, 1993.
- [11] B. Igel'nik, D. Simon, The eigenvalues of a tridiagonal matrix in biogeography. *Appl. Math. Comput.* **218** (2011), no. 1, 195-201.
- [12] E.I. Jafarov, N.I. Stoilova, J. Van der Jeugt, Finite oscillator models: the Hahn oscillator, *J. Phys. A: Math. Theor.* **44** (2011), 265203.
- [13] M. Kac, Random walk and the theory of Brownian motion, *Amer. Math. Monthly* **54** (1947), 369–391.
- [14] R. Koekoek, P.A. Lesky, R.F. Swarttouw, Hypergeometric orthogonal polynomials and their q -analogues, *Springer Monographs in Mathematics*, Springer-Verlag, Berlin, 2010.
- [15] K. Maeda, S. Tsujimoto, A generalized eigenvalue algorithm for tridiagonal matrix pencils based on a nonautonomous discrete integrable system. *J. Comput. Appl. Math.* **300** (2016), 134–154.
- [16] K. Nomura, P. Terwilliger, Krawtchouk polynomials, the Lie algebra $sl(2)$, and Leonard pairs, *Linear Algebra Appl.* **437** (2012), 345–375.
- [17] R. Oste, J. Van der Jeugt, Doubling (dual) Hahn polynomials: classification and applications, *Symmetry, Integrability and Geometry: Methods and Applications* **12** (2016), 003.
- [18] R. Oste, J. Van der Jeugt, A finite oscillator model with equidistant position spectrum based on an extension of $su(2)$, *J. Phys. A: Math. Theor.* **49** (2016), 175204.
- [19] J.J. Sylvester, Théorème sur les déterminants, *Nouvelles Ann. Math.* **13** (1854), 305.
- [20] O. Taussky, J. Todd, Another look at a matrix of Marc Kac, *Linear Algebra Appl.* **150** (1991), 341–360.
- [21] W.C. Yueh, Eigenvalues of several tridiagonal matrices. *Appl. Math. E-Notes* **5** (2005), 66-74.

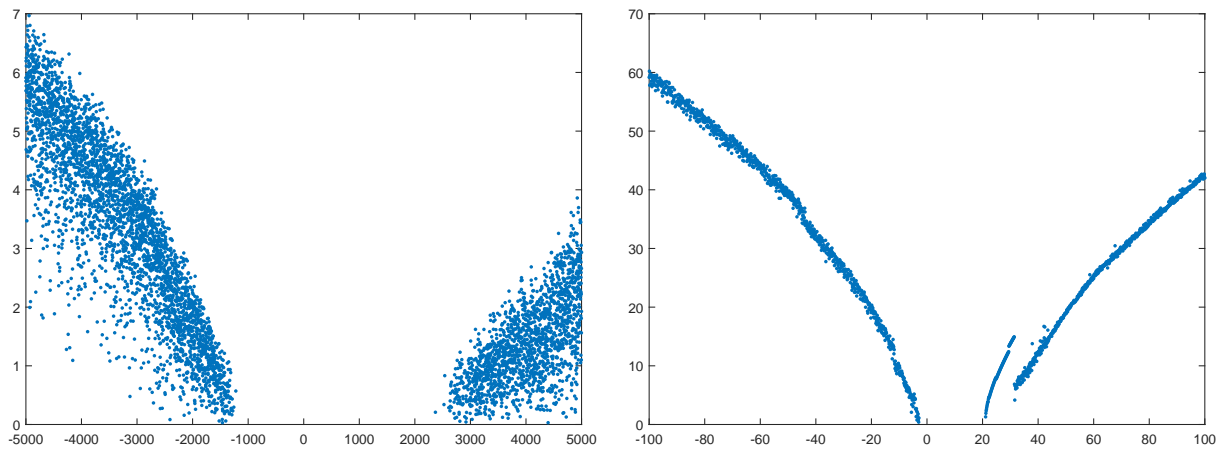


Figure 1: Plots of the largest imaginary part of the computed eigenvalues of $H_n(a)$ (n even and $a = -b$) for different values of a on horizontal axis. On the left for $n = 10$, on the right for $n = 100$.

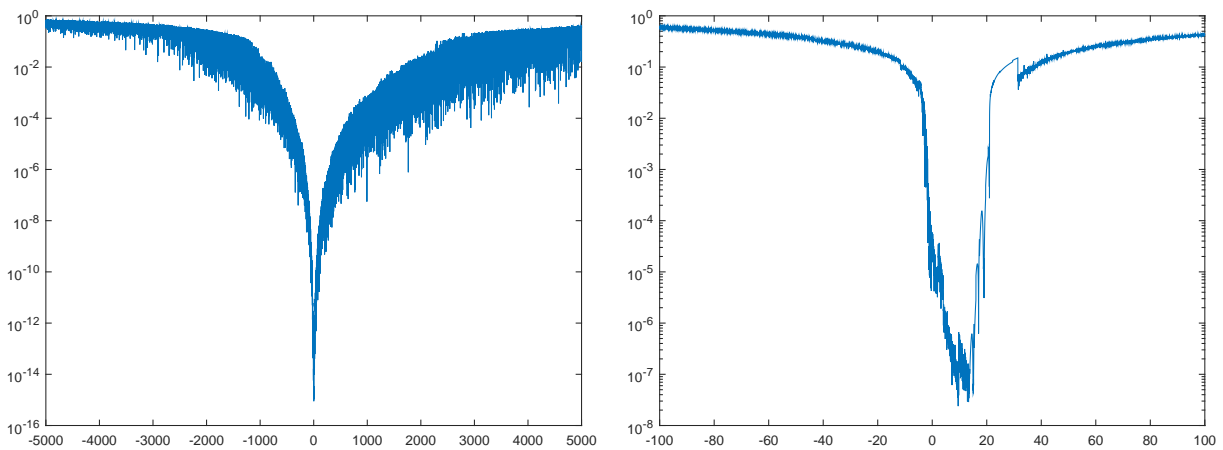


Figure 2: Plots of the relative error in the computed eigenvalues of $H_n(a)$ (n even and $a = -b$) for different values of a on horizontal axis. Left $n = 10$ and right $n = 100$.

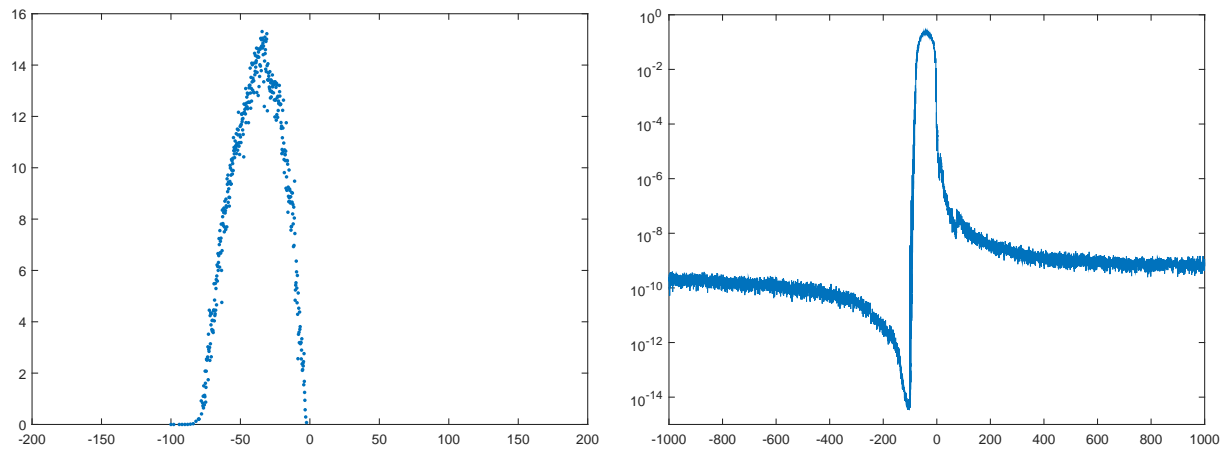


Figure 3: For different values of a as denoted on the horizontal axis, on the left a plot of the largest imaginary part and on the right a plot of the relative error of the computed eigenvalues of $H_{101}(a)$.

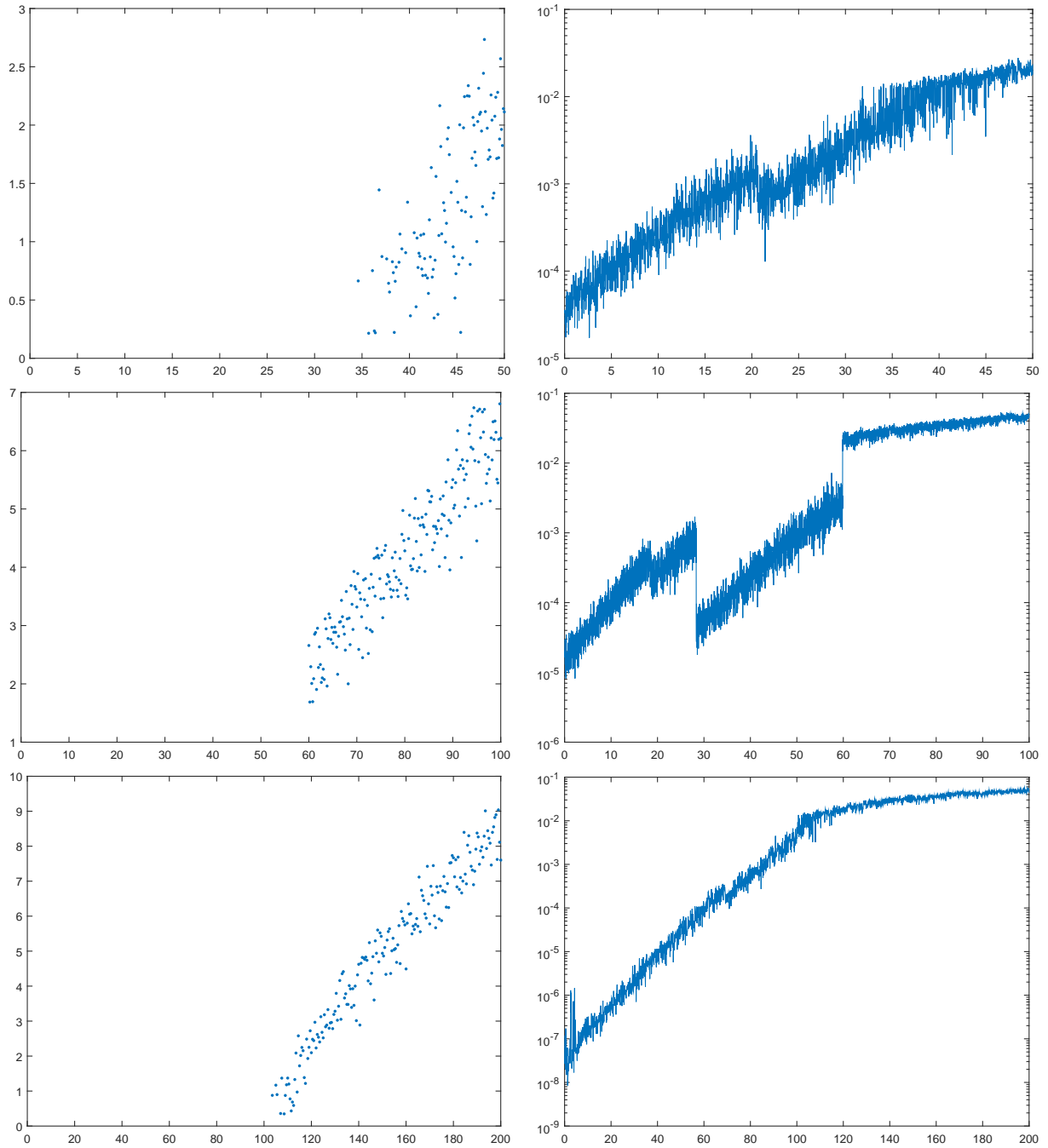


Figure 4: Plots of the largest imaginary part (left) and the relative error (right) in the computed eigenvalues of $H_{100}(a, b)$, horizontal axis varying values of b . Top row $a = 0$, middle row $a = 1$, bottom row $a = 20$.

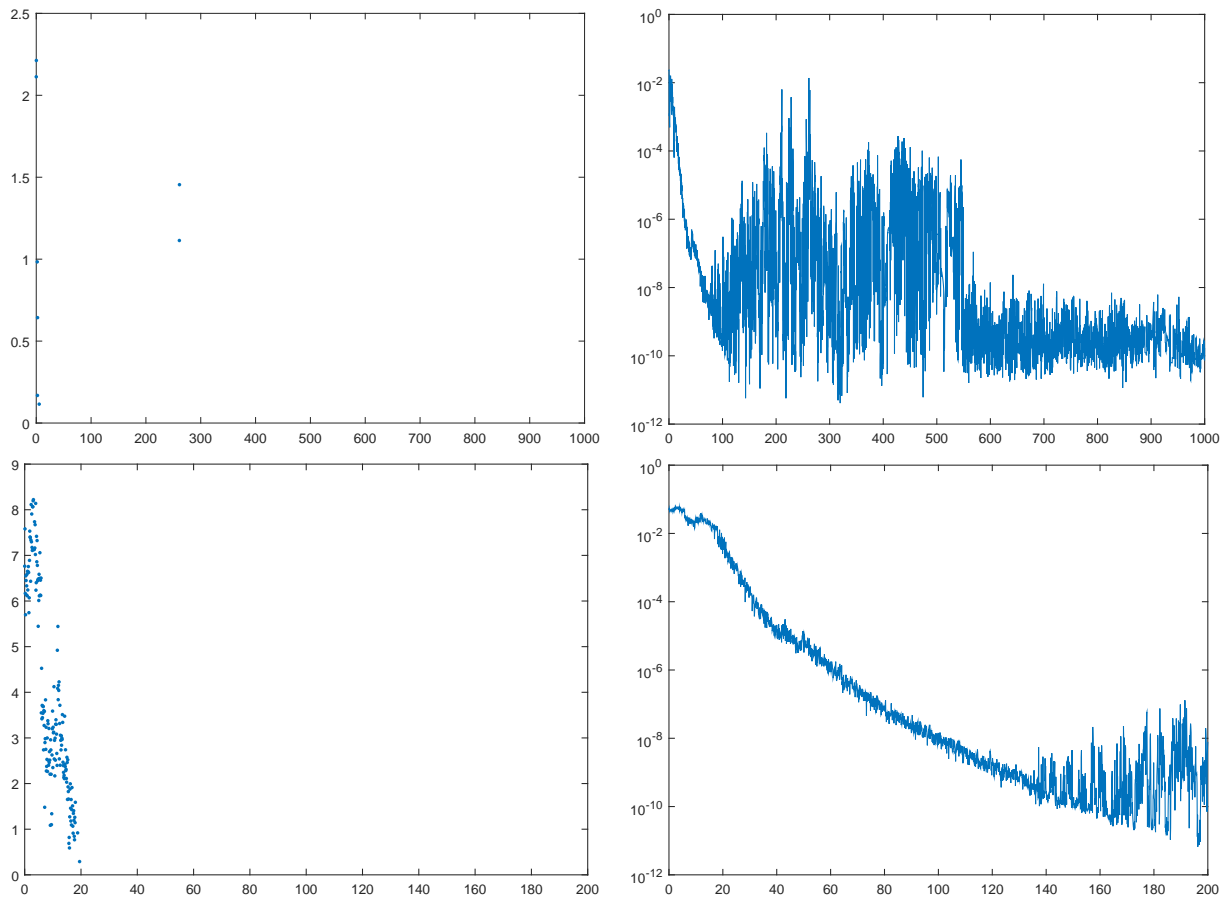


Figure 5: Plots of the largest imaginary part (left) and the relative error (right) in the computed eigenvalues of $H_{100}(a, b)$, horizontal axis varying values of a . Top row $b = 50$, bottom row $b = 100$.

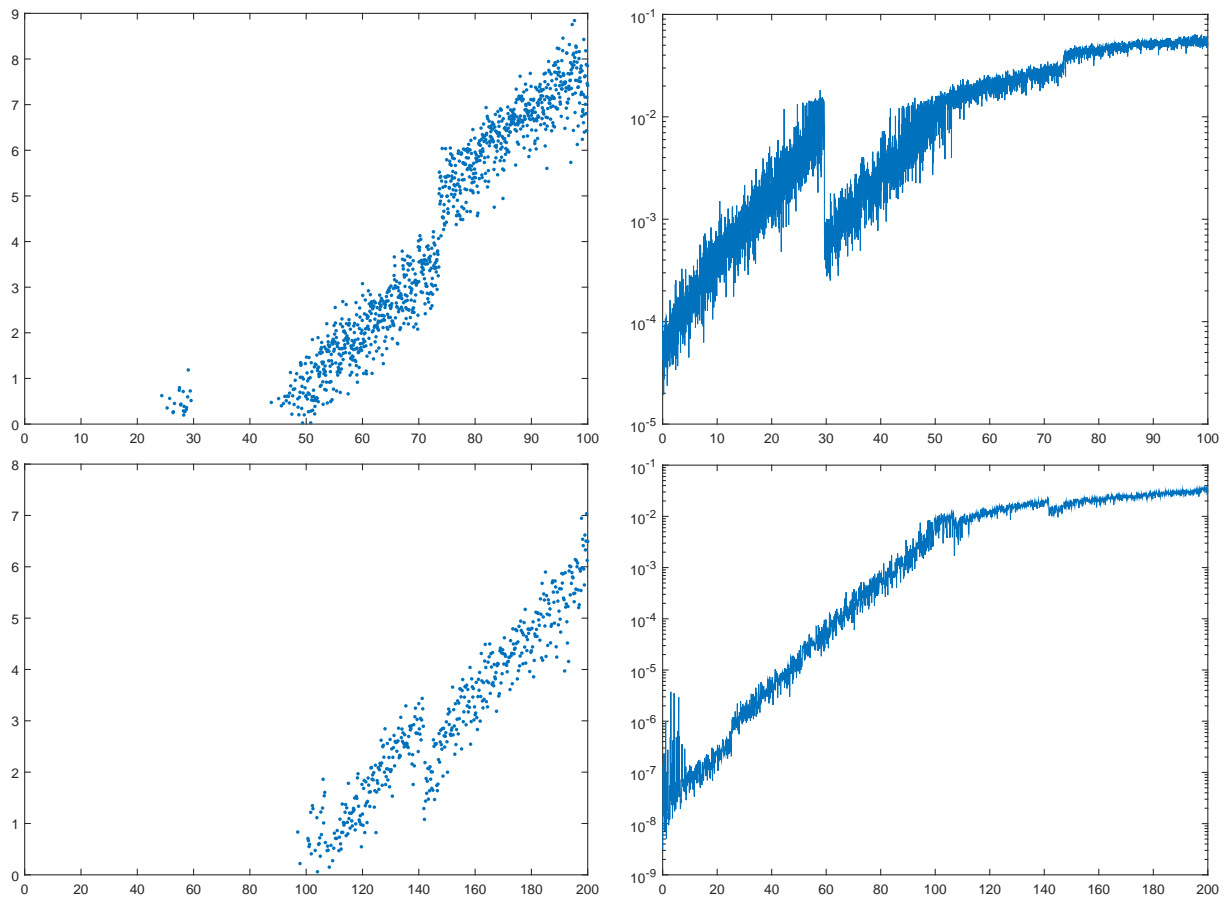


Figure 6: Plots of the largest imaginary part (left) and the relative error (right) in the computed eigenvalues of $H_{101}(a, b)$, horizontal axis varying values of b . Top row $a = 0$, bottom row $a = 25$.